Accepted Manuscript

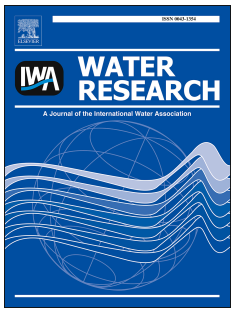

Inorganic fouling mitigation by salinity cycling in batch reverse osmosis

David M. Warsinger, Emily W. Tow, Laith A. Maswadeh, Grace Connors, Jaichander Swaminathan, John H. Lienhard V

PII: S0043-1354(18)30074-5

DOI: 10.1016/j.watres.2018.01.060

Reference: WR 13539

To appear in: *Water Research*

Received Date: 3 October 2017

Revised Date: 23 January 2018

Accepted Date: 25 January 2018

Please cite this article as: Warsinger, D.M., Tow, E.W., Maswadeh, L.A., Connors, G., Swaminathan, J., Lienhard V, J.H., Inorganic fouling mitigation by salinity cycling in batch reverse osmosis, *Water Research* (2018), doi: 10.1016/j.watres.2018.01.060.

Inorganic fouling mitigation by salinity cycling in batch reverse osmosis

David M. Warsinger[a,], Emily W. Tow[a], Laith A. Maswadeh[b], Grace Connors[a], Jaichander Swaminathan[a], and John H. Lienhard V[a,*]

[a.] Rohsenow Kendall Heat Transfer Laboratory, Department of Mechanical Engineering, Massachusetts Institute of Technology, 77 Massachusetts Avenue, Cambridge, MA 02139-4307 USA

[b.] Department of Management Science and Engineering, Stanford University, 450 Serra Mall, Stanford, CA 98305

[*] Corresponding Author; lienhard@mit.edu

Abstract

Enhanced fouling resistance has been observed in recent variants of reverse osmosis (RO) desalination which use time-varying "batch" processes. However, the mechanisms of batch processes' fouling resistance are not well-understood, and models have not been developed for prediction of their fouling performance. Here, a framework for predicting reverse osmosis fouling is developed by comparing the fluid residence time in batch and continuous (conventional) reverse osmosis systems to the induction times of crystallization for sparingly soluble salts. This study considers the inorganic foulants calcium sulfate (gypsum), calcium carbonate (calcite), and silica, and the work predicts maximum recovery ratios for the treatment of typical water sources using batch reverse osmosis (BRO) and continuous reverse osmosis. Experimental validation of this prediction method is demonstrated through observations of the time delay for $CaSO_4$ membrane scaling in a bench-scale, recirculating reverse osmosis unit with trials at varied salinity. The results and implications are organized from scientific to applied. For the most fundamental results, each salt is individually analyzed ($CaCO_3$, $CaSO_4$) for maximum recovery ratio by inlet salinity, shown in contour plots. Next, the maximum recovery ratios

of batch and conventional RO are compared across several water sources, including seawater, brackish groundwater, and RO brine. Due to batch RO's shorter residence times due to the salinity cycling from low to high each batch, significantly higher recovery ratios and higher salinity were possible in batch RO than in continuous RO for all cases examined. Finally, for the most applied case, representative RO brine samples were analyzed for increasing the maximum possible recovery. Overall, the induction time modeling methodology provided here can be used to allow RO to operate at high salinity and high recovery, while controlling scaling. The results show that, in addition to its known energy efficiency improvement, batch RO has superior inorganic fouling resistance relative to conventional RO.

Highlights

- Inorganic fouling (scaling) propensity was modeled for batch and continuous RO
- Predictive framework compares nucleation induction time and residence time
- Each batch, salinity cycles from low to high, yielding very short residence time
- Fouling compared for $CaSO_4$, $CaCO_3$ & silica in seawater, groundwater, & RO brine
- Batch and semi-batch RO enable much higher maximum water recovery ratio and salinity

Graphical Abstract

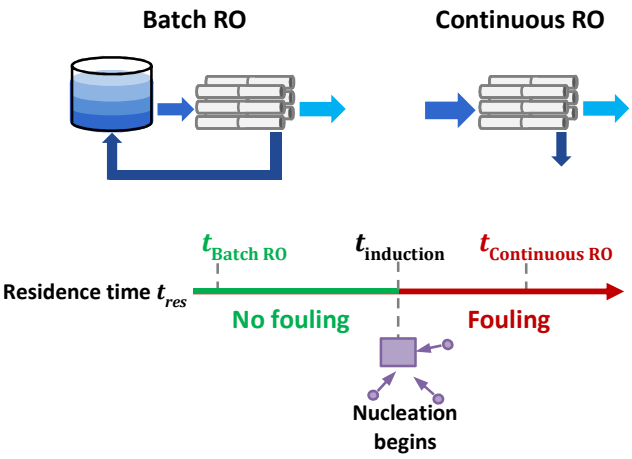

Keywords: Reverse osmosis, batch reverse osmosis, inorganic fouling, nucleation, induction time, high salinity

Nomenclature

1	*time at which supersaturation is reached*
a	*constants for calcium carbonate nucleation induction time*
ind	*induction*
m	*module*
N	*effective number of passes through module*
pass	*passage through the module (ratio of length to feed velocity)*

res	*residence*
t	*time*
T	*temperature*
w	*mass concentration of silica*
BRO	*batch reverse osmosis*
CCD	*closed circuit desalination*
CCRO	*closed circuit reverse osmosis*
LMH	*liter per hour per meter squared*
RR	*recovery ratio*
SI	*saturation index*
TDS	*total dissolved solids*
ZLD	*zero liquid discharge*

1. Introduction

Membrane fouling, such as scaling by salts, is a significant barrier to implementation of water treatment technologies (Rezaei et al., 2017), including the dominant desalination technology, reverse osmosis (RO) (Chakraborty et al., 2015, Shirazi et al., 2010). RO is considered to be particularly vulnerable to scaling in comparison to thermal technologies such as membrane distillation or multistage flash (Tow et al., 2017, Warsinger et al., 2015d, Warsinger et al., 2017c). Despite this, RO is the most widely used and energy-

efficient desalination technology (McGovern and Lienhard, 2014, Thiel et al., 2015, Tow et al., 2015a, Warsinger et al., 2015b), and improving the technology's fouling resistance is critical to the operational efficiency and longevity (Cohen et al., 2017b). Batch systems, rather than continuous systems, offer a new approach for significant fouling and efficiency improvements (Warsinger et al., 2016b). In continuous RO systems, the membrane elements near the end of the train may contact supersaturated solution for extended time periods between cleanings (Greenlee et al., 2009). However, recirculating batch and semi-batch systems periodically flush the concentrated solution out with fresh feed; as a result, no part of the membrane train remains in contact with supersaturated solutions for a prolonged period.

1.1 Batch RO

The term "batch" in this study refers to a desalination process wherein a set quantity of feed solution is concentrated over time up to the required final brine salinity and the process is repeated over multiple cycle times to produce large amounts of permeate. Therefore, batch desalination configurations have time-varying salinity, often achieving this via recirculation to further concentrate a contained volume of fluid (Qiu and Davies, 2012a). In most batch designs, a cycle is used where the recirculating brine is rejected at the end. Batch desalination technologies (Efraty et al., 2011, Qiu and Davies, 2012a) have also shown robust resistance to membrane fouling (Efraty and Septon, 2012), although a theoretical explanation for this is lacking in the literature. These fouling improvements are seen in one of the most rapidly growing technologies, a semi-batch RO process, called CCRO, or closed circuit reverse osmosis (and trademarked as CCD, or closed-circuit desalination) (Stover, 2013). The technology is classified as a semi-batch process because although it cycles salinity over time, it continuously introduces new feed water to the system. The semi-batch design allows for improvement over traditional RO with a similar design and flow parameters, and can be retrofitted into existing systems. Batch RO is expected to have

very similar advantages, with energy improvements over CCRO due to reduced entropy of mixing (Warsinger and Tow, 2016) and slight fouling improvements from reduced residence time at high salinities (Warsinger et al., 2016b). However, the semi-batch design, CCRO, has inefficiencies that batch RO does not. In CCRO but not batch RO, there is continuous mixing between concentrating brine and moderately saline feed. This mixing increases osmotic pressure, increases the time to reach high recoveries, and makes higher recoveries more energy intensive to achieve.

CCRO has been tested to recoveries as high as 97% for brackish waters, although 82-92% is more typical (Stover, 2013): these levels greatly exceed typical RO recoveries of 50-60% (Shirazi et al., 2010).

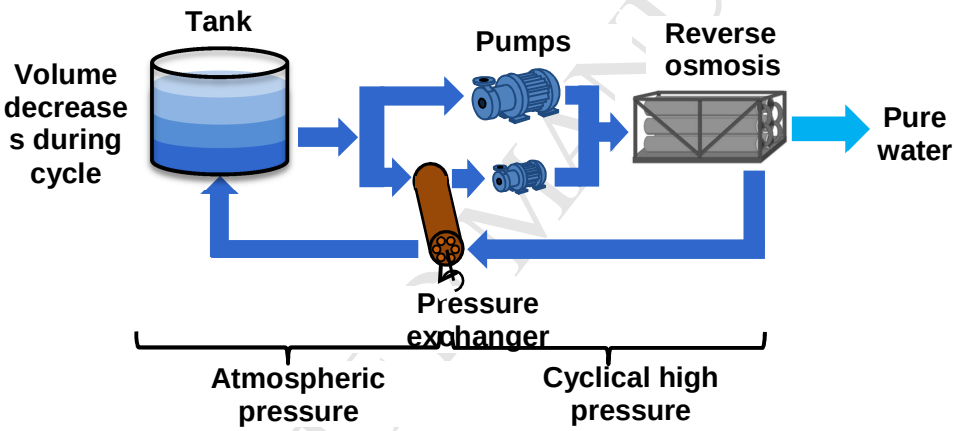

Figure 1. A potential configuration of batch reverse osmosis that uses a pressure exchanger to maintain high pressure in the RO module despite atmospheric conditions in the tank (Swaminathan et al., 2017, Warsinger et al., 2016b).

1.2 Fouling in RO

Fouling occurs when organic, inorganic, or biological water contaminants attach to the membrane (Tong et al., 2017). Fouling on RO membranes reduces permeate flux and quality (Hoek et al., 2008, Salvador Cob et al., 2012), increases the streamwise pressure drop as the feed flows across the membrane, decreases energy efficiency, and leads to more frequent membrane replacement and the need for

extensive pretreatment (Comstock et al., 2011, Malki, 2008, Warsinger et al., 2015e). These effects lead to higher operational costs for an RO facility, which in turn affect water cost. Resistance to fouling of various types including inorganic, organic, and biological has thus been an important long-term focus of research. Inorganic fouling—the accumulation of salts and other inorganic substances, such as silica, on membranes—can be avoided by operating the process under conditions that prevent nucleation of crystals (D. M. Warsinger, 2016, Pomerantz et al., 2006, Warsinger et al., 2015a). Here we show this to be a potentially major advantage of the batch processes compared to conventional steady state RO. Variable conditions like those found in batch processes may also inhibit biofouling (Warsinger et al., 2015e).

The susceptibility of RO membranes to damage by fouling has prompted the development of other processes such as membrane distillation (Rezaei et al., 2017, Servi et al., 2017, Warsinger et al., 2014) and forward osmosis (Boo et al., 2012), which are thought to exhibit greater resistance to fouling (Tow et al., 2017, Warsinger et al., 2017a, Warsinger et al., 2017c, Xie et al., 2015). Furthermore, a trend in environmental legislation mandates for zero-liquid-discharge (ZLD) to reduce pollution from brine waste is requiring many applications to use higher recoveries (Qiu and Davies, 2012b). Additionally, newer RO membranes have focused on increasing permeability and membrane flux to reduce sizes and costs (Cohen-Tanugi et al., 2014), but these higher fluxes, although bounded by the limiting effect of concentration polarization (McGovern et al., 2016), may still lead to increased fouling.

As wastewater reuse increases and the adverse effects of groundwater salinity on agriculture continue to grow (Cohen et al., 2017a), RO is increasingly being used for water sources other than seawater (Kumar et al., 2017). At higher recovery ratios of brackish water, inorganic fouling has a greater impact on system performance. High concentrations of common dissolved ions such as Ca^{2+}, SO_4^{2-}, and CO_3^{2-} are also significant factors in system fouling. Khan et al. (Khan et al., 2014) harvested foulant layers from RO membranes used to treat seawater and secondary wastewater effluent in a pilot plant, and found that,

1 although organic foulants dominated in seawater RO and on the first membrane of wastewater RO,
2 inorganic foulants comprised 88.9% by mass of the foulant layer on the last membrane in the
3 wastewater RO train. Some sparingly soluble salts common in the scaling of desalination systems are
4 listed in Table 1. For these solutions, $CaCO_3$ and $CaSO_4$ are the most common fouling concerns in typical
5 desalination systems (Comstock et al., 2011, Jawor and Hoek, 2009, Yang, 2005). Solubility is calculated
6 using PHREEQC software (Parkhurst and Appelo, 2013), using the PHREEQC database for activity
7 coefficients and data from a variety of sources on the standard state ion concentration (Thiel and
8 Lienhard, 2014).

9 Scaling mitigation can involve reducing supersaturation through pretreatment, prolonging the induction
10 time through antiscalant addition (Shirazi et al., 2010), or—as proposed in the present study—keeping
11 the residence time of supersaturated solutions under the nucleation induction time.

12 **Table 1.** Solubility of common inorganic foulants at 25 °C, calculated with PHREEQC (Kempter et al., 2013,
13 Parkhurst and Appelo, 2013)

Salt	Name	Solubility[g/L]	Solubility Product K (275°)	Solubility reduced by:
$CaCO_3$	Calcium carbonate (Calcite)	0.29	-8.48	High temperature, high pH
$CaSO_4$	Calcium sulfate (Gypsum)	2.0	-4.58	Very high temperature
SiO_2	Silica	0.18	-	High temperature

14

15 Knowledge of crystallization kinetics can be used to avoid or minimize scaling under supersaturated
16 conditions. Crystallization is delayed for a period of time known as the nucleation induction time, which

is the time needed for stable crystals to form under given conditions (Çelikbilek et al., 2012, Warsinger et al., 2017c). This delay occurs because very small nuclei (of a few hundred atoms) are unstable in supersaturated conditions due to competition between the interfacial energy of the crystal surface and the change in Gibbs energy of the solid relative to the salt in solution (Çelikbilek et al., 2012, Nagy and Braatz, 2012).

1.3 Fouling in batch and semi-batch RO

Applications of batch and semi-batch RO have demonstrated impressive fouling resistance. Stover (Stover, 2012) has proposed that CCRO can reduce fouling and scaling through the time-variation of water composition at the membrane. Tarquin and Delgado (Tarquin and Delgado, 2012) reported that batch RO may be especially resistant to fouling and scaling based on experiments in which fouling was not observed even with brackish water under high concentrations of silica and calcium sulfates at 90% recovery. Several studies have shown CCRO to be resistant to silica fouling (Sonera et al., 2015). In one such study, the system began at around half saturation (57 ppm with a pH of 5.5) and went to 93.8% recovery without any evidence of silica fouling. Notably, an antiscalant was used, but antiscalants largely delay nucleation, rather than alter saturation levels (Shirazi et al., 2010). Another CCRO study began at around one quarter of silica saturation (32 ppm) and went to 96% recovery without any evidence of fouling (Gal et al., 2016). A third study began near saturation (>125 ppt) with 85% recovery (Efraty, 2015); slight flux decline was observed over 23 minutes of run time. CCRO plants that begin with supersaturated foulants such as silica have exhibited heavy fouling (Efraty, 2015). The trend seems to be that, even for systems that concentrate past saturation, fouling is minimal if the starting feed is subsaturated. This observation hints that frequently returning to sub-saturated concentrations may be the key to avoiding fouling, and modeling the mechanism behind any fouling that does occur will allow the system to advance the limits of adverse fouling conditions with scientific rigor and precision.

A substantial advantage that batch and semi-batch processes have over traditional steady flow RO is their transient operation, or the limited time of supersaturated operation. Periodically, they eject all of the brine and refill the system with feed water. As long as no crystals have yet formed and the feed is subsaturated, progress toward nucleation should be undone at the end of each cycle when brine is rejected from the system (Warsinger et al., 2015c). Crystals that have formed may also dissolve. In contrast, continuous RO operates at steady state, so high salinity stages for higher recovery operations may run at supersaturated conditions almost indefinitely, causing fouling (Bartman et al., 2011, Chai et al., 2007). The long times of supersaturation in continuous RO are only interrupted by periodic cleaning processes, which can be as infrequent as weeks or months in industrial applications. Notably, batch RO has an additional advantage not discussed here: batch cycles have a natural osmotic backwash step after each cycle, and osmotic backwash (Ramon and Hoek, 2012, Sagiv et al., 2008, Tow et al., 2016) and flow reversal (Bartman et al., 2009, Gu et al., 2013) have proven to be effective antifouling mechanisms in continuous RO because they can remove and dissolve crystals.

In this paper, we contrast the cycle time of batch RO to the maximum residence time in continuous RO. These times are compared to the nucleation induction time, to get an estimate of what recovery ratios and salinities can be tolerated before scaling occurs in either system. An expression for residence time in batch and semi-batch systems is developed, and nucleation induction time is correlated from existing measurements for common scalants ($CaSO_4$, $CaCO_3$). This is displayed as colored contour plots of fouling zones as a function of inlet feed salinity and recovery ratio, which include batch and continuous RO paths. The use of nucleation induction time to predict the time delay for scaling in RO is validated by experimental data for calcium sulfate solutions. The methods are applied to key water types (seawater and groundwater), and examined for extending recovery for representative RO brine. Notably, these results provide upper bound salinities for extreme fouling conditions, as membranes themselves may play a role in promoting the nucleation of foulants (Elimelech et al., 1997).

2. Modeling methodology

The system residence time is defined as the time the portions of the feed solution at highest supersaturation remain in the system. The other relevant timescale is the nucleation induction time for salt crystals—the time required for stable crystals to form in a supersaturated solution—which can range from minutes to days depending on the supersaturation and other conditions (Chesters, 2009). Once the system residence time reaches the induction time, inorganic crystallization is predicted. This study predicts fouling by matching these times. For this calculation, conditions in the bulk solution are used in established correlations for the induction time of foulants of primary concern.

If systems are run transiently, batch cycle times may be shorter than the times for nucleation induction of common foulants, such as $CaSO_4$ and $CaCO_3$ (Pomerantz et al., 2006)]. As a result, systems starting operation at sub-saturated conditions may be able to run up to concentrations several times saturation without seeing crystallization. To determine whether fouling is likely to occur, the length of time over which the feed is supersaturated in an RO system is compared to the nucleation induction time, which is calculated from feed concentration using existing correlations(He et al., 1994, Xyla et al., 1992). Figure 2 illustrates this comparison.

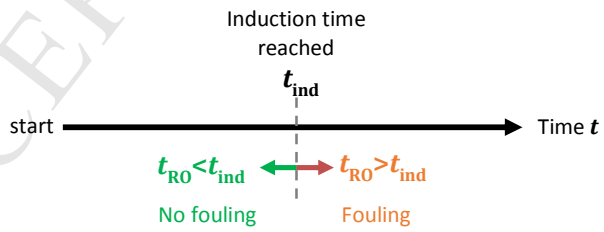

Figure 2. Timeline relating system times to fouling prediction. Whether fouling occurs can be determined by comparing the induction time (t_{ind}) for the salt at a representative (worst-case) concentration to the residence time (t_{RO}) of water remaining in the system.

2.1 Nucleation induction time

In this section, we report or develop correlations for the nucleation induction time for three common scalants: $CaCO_3$, $CaSO_4$, and silica. Although these induction times are derived from experiments in stirred liquids (with stirrer bars and recirculating baths (He et al., 1999), we assume that they apply to the moving fluids in RO systems. The same assumption enabled successful prediction of scaling in membrane distillation systems in our previous report (Warsinger et al., 2017c).

These correlations are based on the assumption of pure salt solutions in which pH is determined by concentration. To include the effects of pH in real waters, the saturation index (SI) used in the induction time correlations is calculated using PHREEQC for each solution's composition and pH. However, additional impacts of pH and the presence of other species on induction time are not accounted for in the present model due to the lack of available data on these effects.

2.1.1 Calcium carbonate

The nucleation induction time of $CaCO_3$ was calculated using a correlation from Refs. (He et al., 1999, Xyla et al., 1992):

$$t_{\mathrm{ind,CaCO_3}} = 10^{\left(a_1 + \frac{a_2}{\mathrm{SI}} + \frac{a_3}{T} + \frac{a_4}{\mathrm{SI}\,T}\right)}, \quad (1)$$

where t_{ind} is the induction time, SI is the saturation index , T is the absolute temperature (in K), and the empirically determined constants are as follows: a_1 = 4.22, a_2 = -13.8, a_3 = -1876.4, and a_4 = 6259.6.

2.1.2 Calcium sulfate

The nucleation induction time of calcium sulfate as gypsum ($CaSO_4{\cdot}2H_2O$) was calculated using linear interpolation within Table 1 of Ref. (He et al., 1994) for the data at 25 °C. To predict induction times at

higher or lower supersaturation than tested by He et al. (1994), extrapolation was performed with a power-law fits of the data:

$$\begin{aligned} t_{\mathrm{ind,CaSO_4}} &= 55.5\ \mathrm{SI}^{-4.701} \qquad \mathrm{SI}<0.20 \\ t_{\mathrm{ind,CaSO_4}} &= 47.4\ \mathrm{SI}^{-4.858} \qquad \mathrm{SI}>0.66 \end{aligned} \tag{2}$$

2.1.3 Silica

Silica induction time data is limited, so we fit a correlation to experimental observations of the delay in static and dynamic light scattering from supersaturated silica solutions reported in Ref. (Kempter et al., 2013):

$$t_{\mathrm{ind,SiO_2}} = 7.93\mathrm{x}10^{18}\ w^{-5.57} \tag{3}$$

where $t_{\mathrm{ind,SiO_2}}$ is the induction time in seconds and w is the mass concentration of silica in mg/L.

2.2 Modeling groundwater

Groundwater is highly variable in nature, and thus no representative numbers for ion concentrations are easily available. To describe "average groundwater," first median salt concentrations were taken from the entire dataset produced by the US Geological Survey, which contains over 120,000 samples (Qi and Harris, 2017). Additionally, the standard deviations of concentrations were taken from this dataset and added to the medians for a higher-fouling case. Second, for both these two sets of concentrations, the nearest real sample of groundwater was used, which was determined by comparing the concentrations of Ca^{2+}, SO_4^{2-}, Cl^-, Na^+, Mg^{2+}, and HCO_3^{2-} (Gutentag et al., 1984) with a least squared fit, weighted for the fouling salts studied here. To predict nucleation in these sources, the SI's were calculated in PHREEQC for the scaling salts at five different recovery ratios, and a curve-fit for these points was used in the SI

input to the equations described above. This fit was used as input data for the further calculations in the contour maps.

Table 2. Average groundwater composition calculated from the US Geological Survey (Qi and Harris, 2017)

Ion	Average groundwater	Average groundwater + 1 standard deviation
Na^+	40.1	2200
K^+	3.08	15
Ca^{2+}	45.8	170
SO_4^{2-}	35	510
CO_3^{2-}	248.9	539.0
Cl^-	7.19	3200
F^-	0.44	0.7
Mg^{2+}	12.7	58

2.3 Residence time in RO systems

The residence time for steady RO is very long relative to batch processes. Notably, since the initial nucleation causes a cascade of crystal growth from the first crystals (secondary nucleation), nucleation induction time must be calculated from the worst-case parts of an RO module, which can be difficult. Because steady RO is a continuous process, the time period during which parts of the membrane are exposed to supersaturated conditions is long, and can be estimated in several ways (Shirazi et al., 2010). One calculation for this supersaturation time is examining the residence time of solutes near the membrane. The maximum residence time in typical RO modules considering boundary layers at the membrane surface (as derived in our previous report (Warsinger et al., 2017c) was found to be several days. This residence time calculation used a methodology that considered module length, and the boundary layer velocity at a distance from the wall that is related to the minimum size for stable

crystals. However, for practical systems, a more realistic maximum residence time may consider the various stagnant regions in the RO system due to feed spacers and pressure vessel end/entrance geometries. Such areas are only effectively purged of nucleating crystals during cleaning cycles. Consequently, the residence time for continuous RO can be estimated by the time between cleaning processes when the supersaturated solution in these dead zones is removed. Cleaning can occur as frequently as once a week, but are often less frequent (Shirazi et al., 2010).

Based on these considerations, for the purpose of comparing batch and continuous processes, a residence time of about 1 week is used for continuous RO in the results of Section 2.3. Irrespective of the precise value selected, the residence time of the continuous RO processes is much greater than that of the batch process because the cycle time of a batch process is only a few minutes (Waly et al., 2009, Warsinger et al., 2017c).

For batch processes, the residence time is considered to be the process cycle time as an upper limit estimate. The residence time for the batch and CCRO systems is:

$$t_{\mathrm{res}} = t_{\mathrm{pass}} N_{\mathrm{pass}} = t_{\mathrm{pass}} \frac{\mathrm{RR}}{\mathrm{RR}_m (1-\mathrm{RR})}, \qquad (4)$$

where t_{res} Is the residence time, t_{pass} is the time for a unit of fluid to complete one pass through the module (i.e., the ratio of length to feed velocity), RR is the recovery ratio for a complete cycle, RR_m is the recovery ratio from one pass through the module, and N_{pass} is the effective number of passes through the module.

The bulk salinity in the system can be compared with time, as the batch RO system is modelled (Figure 3). Note that the concentrations calculated for batch RO induction times are calculated at the maximum concentration to give very conservative antifouling predictions.

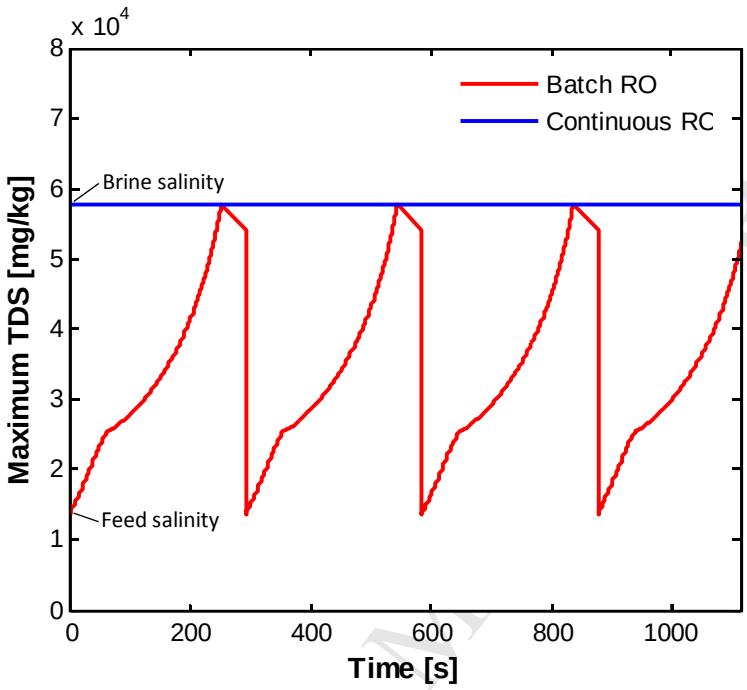

Figure 3. Batch RO salinity varies cyclically, reducing the amount of time the last membrane element spends in contact with highly-supersaturated solution.

2.4 Predicting fouling by comparing induction and residence times

Prediction of fouling remains a significant challenge due to the complexity of fouling phenomena, the stochastic nature of fouling, and the very long times needed to experimentally gather data (often months for one data point). While exact prediction of fouling behavior is generally not possible, inorganic fouling is better understood than other types, and models built from experimental data can yield useful insights despite variability in real conditions.

The nucleation of salts, or inorganic fouling, is described by classical nucleation theory; and Eqns. (1), (2), and (4) provide empirical fits to the expected behavior for each foulant. These equations describe nucleation in stirred cells, and focus on nucleation in the fluid bulk. Such conditions are very similar to the fluid bulk in an ideal RO setup, with minor geometric differences in flow patterns. Data is not available for systems whose salinity varies over time as in batch RO: however, a conservative case for batch systems using the worst salinity can still be added to such plots.

Contour maps describing fouling can be created using these nucleation equations and residence times in RO and batch RO systems. The time axis for these maps describes sufficient time for nucleation of salts. This time can be compared with the typical residence times of volumes of water within these systems. These maps can visually show conditions of significant fouling, mapped by time, inlet salinity, and final recovery. The RO technology residence times can be plotted on these contour maps: where a technology crosses the fouling region, significant bulk nucleation is expected.

In practice, predicting fouling occurrence is very hard to do, as other constituents impact fouling (e.g. interaction with biofouling, interactions with suspended matter, interactions with steel surfaces). Antiscalants, pH modification, and other mitigation methods also have influence. The goal is thus to use quantitative modelling for to gain *qualitative* insights: just how much does fouling differ between batch and continuous RO? As seen in other fouling experiments, while the values shown here may be accurate for experiments of pure solutions, they likely will differ for real solutions in industrial settings. Nevertheless, using the methodology here with experiments of a given water source to determine induction time, individual maps can be made.

3. Results

3.1 Experimental validation of theory

Although induction time correlations were derived from experimental data, the relationship of nucleation induction time to the time delay before scaling in RO has not been previously validated. Our previous reports (Tow et al., 2015b, Tow et al., 2017, Warsinger et al., 2016a) include measurements of flux decline due to $CaSO_4$ scaling in a recirculating bench-scale RO system, which can be used to validate the theory developed in the present work. A custom-designed 8 cm-long, 3 cm-wide, 1 mm-deep cross-flow module was used with Dow SW30HR RO membranes to filter supersaturated $CaSO_4$ solutions at constant pressure for 36 hours or until fouling had clearly occurred. The supersaturated $CaSO_4$ solutions were created by mixing sodium sulfate and calcium chloride solutions; sodium and chloride are therefore also present at twice the $CaSO_4$ concentration. Temperature was maintained at 20±1 °C with a temperature controller. Feed concentration was maintained within ±5% of the value stated in Table 3 by periodically diluting the feed solution as it became more concentrated. Pressure was controlled with a back pressure regulator, and chosen such that different trials had approximately the same initial flux.

Flux was measured by recording the mass of permeate on a digital balance and calculating the rate of change over 15-minute increments. Flux declined slightly in all trials due to membrane compaction, but the flux decline rate was independent of feed concentration for the trials that had no fouling during 36 h. For the trials with fouling, flux declined significantly more than in the trials without fouling (at least 20% over 36 h). The time of onset of fouling was estimated from the flux decline data as the time when the flux decline curve diverged from the slight flux decline observed in the non-fouling trials. Fouling and non-fouling results were confirmed by visually examining used membranes; significant crystallization was observed only in trials with significant flux decline. For details of the experimental data collection, see (Tow et al., 2015b, Tow et al., 2017).

Theoretical predictions and experimental measurements of fouling onset time are given in Table 3 (Tow et al., 2015b). The predictions in Table 3 considered both the concentration in the bulk and the higher concentration at the membrane (a result of concentration polarization(Kim et al., 2009); see (Tow et al., 2017 for details of calculations) to calculate upper and lower bounds on induction time, respectively.

Table 3. Time delay of $CaSO_4$ fouling on RO membranes: experimental data from Ref. (Tow et al., 2015b, Tow et al., 2017) and model predictions (Sec. 2.1.2). For reference, the saturation concentration of $CaSO_4$ (as gypsum) at 25 °C is 2.22 g/L in the presence of twice its concentration in NaCl.

Bulk feed concentration [g/L]	Initial flux [LMH]	Concentration near membrane [g/L]	Measured fouling time [h]	Predicted fouling time range [h]
3.99	19.3	6.02	<3	0.57–6.3
3.23	19.7	4.90	13	1.5–85
2.94	19.7	4.48	n/a (>36)	3.2–490
2.65	19.7	4.06	n/a (>36)	5.3–810
2.10	19.4	3.16	n/a (>36)	115–∞*

*Fouling not predicted due to sub-saturated feed.

As expected, the experimental measurements of fouling time delay in Ref. (Tow et al., 2015b, Tow et al., 2017) fall within the range of nucleation induction times in the bulk feed and in the more concentrated solution near the membrane. In the two experimental trials in which fouling occurred, the time delay of fouling occurred between the lower and upper bounds of the model prediction (with and without concentration polarization, respectively). In the three trials in which fouling did not occur, the upper bound of the model prediction was greater than the duration of the experiment (36 h). The difference

between the two bounds on the predicted fouling time is very large, and future studies should elucidate the role of concentration polarization in determining the delay before fouling. However, the success of the model in bounding experimentally-measured fouling time delays helps to validate the use of induction time correlations to predict the time delay of fouling in RO.

3.2 Contour maps for fouling prediction

The RO technologies' residence times can be plotted on fouling contour maps of fouling induction time, with axis for recovery ratio and residence time. The contours represent fouling occurrence colored by different initial saturation indexes. Where a technology line crosses a fouling region (induction time curve for a given feed inlet salinity), significant bulk nucleation is expected to occur. The intersection of the technology lines with a given region (e.g., the batch RO line with the shaded region for an SI of 0.5) give a maximum recovery possible before significant fouling. Notably, batch and semi-batch technologies have the same residence time and are included together.

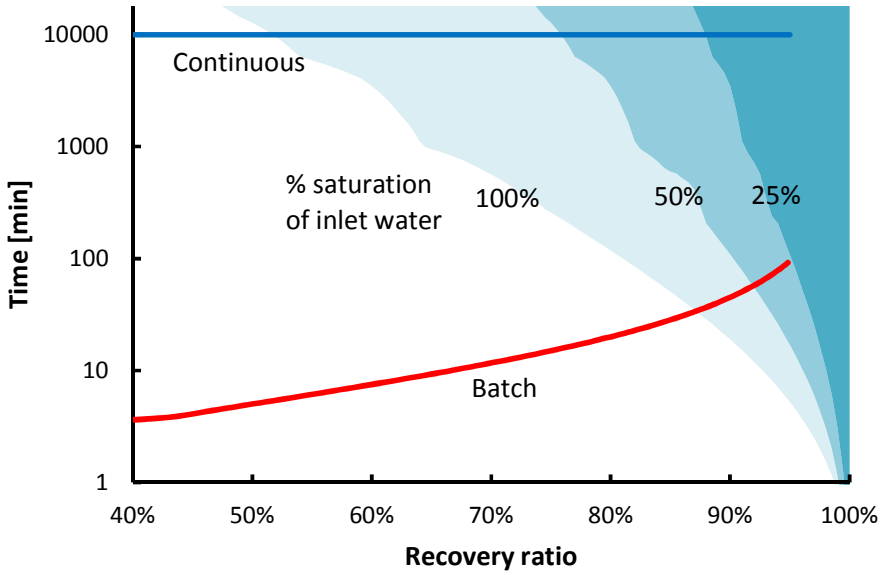

Figure 4. A contour map for gypsum ($CaSO_4$) nucleation induction times, overlaid with curves for residences times of continuous RO and batch RO[1].

The induction times for gypsum (the least soluble form of $CaSO_4$, calcium sulfate dihydrate) are shown in Fig. 4. Continuous RO is expected to begin fouling at moderate recovery ratios (~54%) for saturated solutions, and at about 77% for feed solutions at half of that concentration. Meanwhile, batch RO processes are expected not to foul until about 87% for saturated solutions, and above 90% for feed salinity starting at half the saturation concentration, allowing for most of the operation range to be accessible.

[1] The jagged appearance of the curves at longer induction times is due to the fact that induction time is interpolated from experimental data in Ref (He et al., 1994)(He et al., 1994). For shorter induction times, curves are extrapolated from the data using an exponential fit.

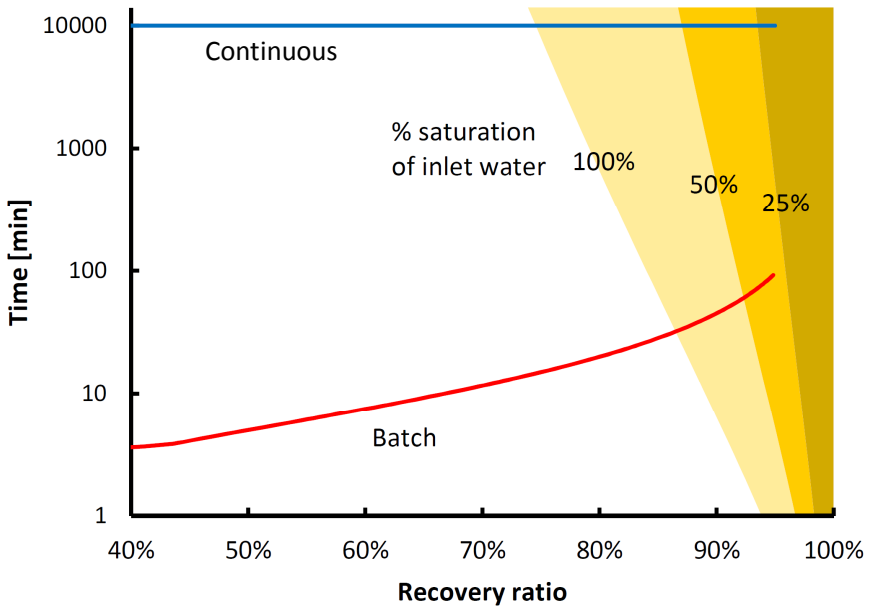

Figure 5. A contour map for calcite ($CaCO_3$) nucleation induction time, overlaid with curves for residences times of continuous RO and batch RO.

As seen in Fig. 5, $CaCO_3$ has relatively long induction times, and is near saturation in many groundwater resources (Gutentag et al., 1984). Given the lengthy induction times for calcite, batch systems are expected to offer less of an advantage over conventional RO for this salt compared to gypsum.

In Figs. 4-6, bulk nucleation occurs at a lower recovery ratio for continuous RO compared to the batch technologies. For example, for gypsum entering near saturation, continuous RO with weekly backwash or cleaning will foul when the recovery has reached 53%, but batch RO will not experience bulk precipitation until the recovery ratio is 87%. Similarly, for $CaCO_3$ beginning at half the saturation concentration, continuous RO will experience bulk nucleation at a recovery of 90% while the batch systems will not see it until 93%. Given the vastly shorter residence times and repeated subsaturated conditions, it is possible that batch RO variants can deal with much more saline brines. After each cycle,

the return to subsaturated conditions may tend to dissolve any crystals that formed on surfaces during previous cycles.

This same data can also be shown very conveniently in terms of the maximum recovery ratio achievable for each salt as a function of initial feed concentration (Figure 6). The maximum achievable recovery ratios is much higher for batch systems than continuous systems.

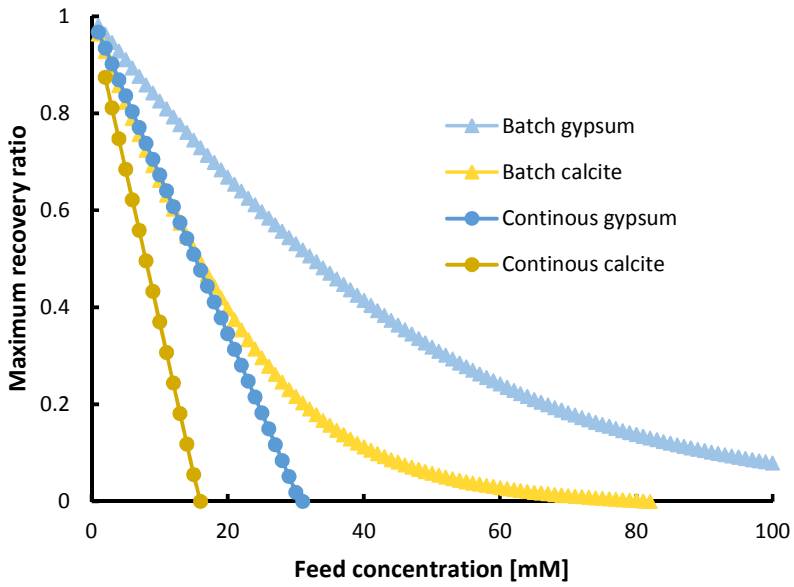

Figure 6. Maximum recovery ratio as a function of feed concentration for $CaSO_4$ and $CaCO_3$ for both batch and continuous RO.

3.3 Implications for RO treatment of real feed waters

In this section, realistic mixed salt solutions are considered, rather than the pure salt solutions discussed in the previous section. Here, the above models are applied based on the inlet concentrations of representative water sources (Table 4). This includes seawater and average groundwater (Gutentag et al., 1984). Here, graphs are provided for maximum recovery before bulk fouling occurs. They include

breakdowns by salt and water source. Instead of displaying both residence times and induction times as in previous sections, the present section sets the operating time (the cycle time in batch RO or the time between cleanings in continuous RO) equal to the induction time to examine the maximum recovery ratio before fouling. These graphs provide insight into conditions where batch can significantly reduce fouling. The ion concentrations used as input for each water source and their calculated saturation indexes are given in Table 4. The modeling for these solutions included the ions Na^+, K^+, Cl^-, F^-, Ca^{2+}, Mg^{2+}, SO_4^{2-}, and CO_3^{2-}.

Table 4. Concentrations of common fouling ions and calculated saturation indexes in different water sources (Qi and Harris, 2017, Roy et al., 2017).

	Concentration (mg/L)			Saturation index	
	Ca^{2+}	$HCO3^-$	$SO4^{2-}$	Gypsum ($CaSO_4 \cdot 2H_2O$)	Calcite ($CaCO_3$)
Seawater	400	140	2650	-0.62	-0.48
Average groundwater	63	251	32	-2.09	-0.32

Notably, these results neglect impacts of concentration polarization, which would further reduce the maximum recovery ratio achievable (Hydranautics, 2001).

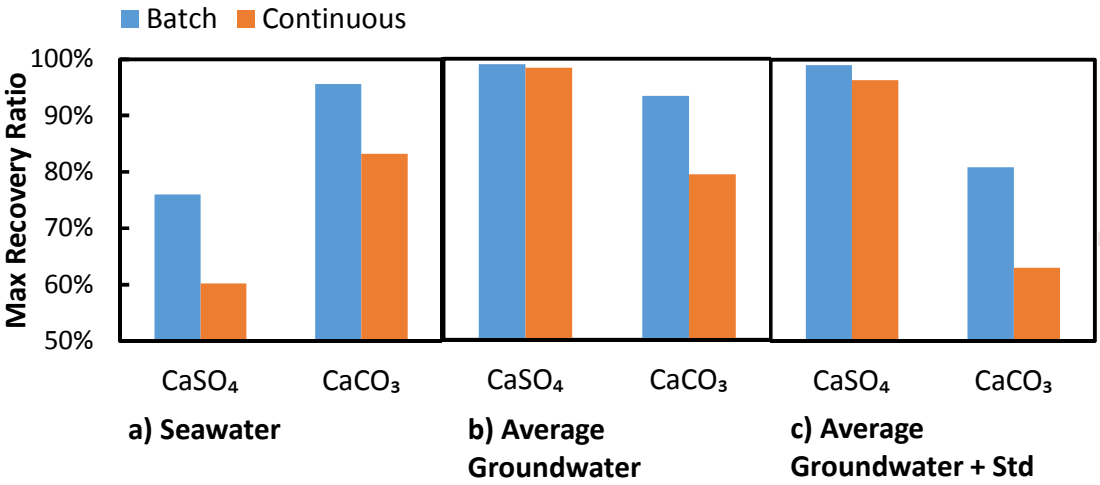

Figure 7. Model results for maximum recovery ratio that avoids fouling with two common salts and three water types a) Seawater, b) groundwater, and c) groundwater with salt concentrations a standard deviation above the US average

As seen in Fig. 7, possible recovery ratios vary significantly by ion, and to a lesser degree, by water type. Unsurprisingly, $CaCO_3$ is the primary salt of concern for groundwater. $CaSO_4$ begins becoming a concern for groundwater with a standard deviation higher concentrations (Fig. 7c), though $CaCO_3$ still dominates due to its lower solubility, and high typical CO_3^{2-} concentrations. Meanwhile, both salts are a concern for seawater, with $CaSO_4$ fouling first under these conditions. For the solutions given, batch systems significantly improve the maximum recovery ratios achievable before bulk nucleation. Notably, these predictions indicate that seawater RO solutions will be saturated with $CaCO_3$ when the recovery ratio reaches around 50%, but fouling is not predicted until much higher recovery ratios due to its long induction time. In practice, fouling is significantly altered by pH changes, chemical softening, and routine use of antiscalants. Additionally, concentration polarization causes supersaturation near the membrane, and hence attainable bulk recoveries will be lower than those shown in Fig. 7.

Overall, despite its low salinity, the composition of this representative groundwater makes it prone to fouling, especially with $CaCO_3$. In contrast, seawater feeds are more prone to $CaSO_4$ fouling. Increasing water recovery from groundwater RO brine is possible with batch RO, due to the higher potential recoveries.

Many RO systems have to limit water recovery in order to avoid scaling. However, it may be possible to recover additional water by feeding a batch RO system with the RO concentrate from an existing continuous RO plant (Figure 8). This approach is predicted to have cost savings compared to conventional treatment for high fouling waters, and is predicted to be cheaper than even continuous RO in most conditions (Warsinger et al., 2017b).

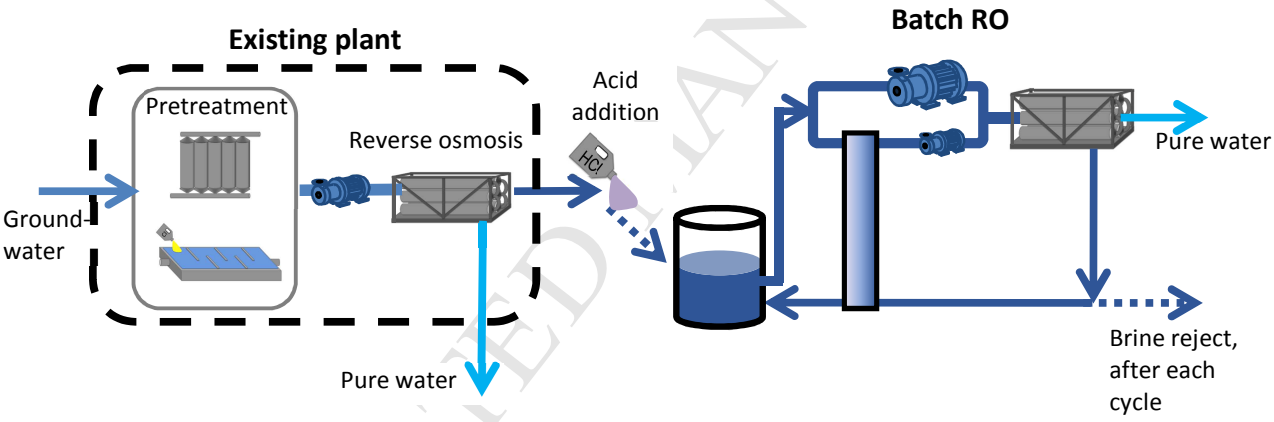

Figure 8. Batch reverse osmosis (combined with acid addition for $CaCO_3$ scaling) can be used to enhance the recovery of traditional continuous reverse osmosis.

To explore this ability, representative samples of inland brackish RO plant concentrate (The U.S. Environmental Protection Agency and Water Research Foundation, 2017) are shown in Table 5. Both concentrates are supersaturated with calcite, but HCl addition to reduce the concentrate pH to 5 is sufficient to create sub-saturated conditions throughout the subsequent batch RO step.

Table 5. Composition of two representative samples[2] of groundwater RO plant concentrate. (The U.S. Environmental Protection Agency and Water Research Foundation, 2017)

Concentrate sample	A	B
Existing RO plant recovery	75%	82.5%
Calcium (mg/L)	1079	718
Magnesium (mg/L)	260.6	199
Potassium (mg/L)	25.7	74
Sodium (mg/L)	774	3327
Bicarbonate (mg/L)	809	379
Chloride (mg/L)	2953	6271
Sulfate (mg/L)	489	1493
SiO_2 (mg/L)	154	201
TDS	6652	13039
pH	7.7	7.9

Using the induction time correlations given in this paper and a model of batch RO salinity[3] as a function of time (Swaminathan et al., 2017), induction time was calculated as a function of time for batch concentration of both water samples. Figure 9 shows how the induction time of silica and gypsum varies over the duration of one cycle of batch RO treating the RO concentrate of Samples A and B. In Sample A, gypsum is the more likely scalant, and the recovery ratio (58%) is chosen such that the cycle time is just

[2] Water compositions specified by a competition for treating high-fouling waters: the US Bureau of Reclamation's More Water Less Concentrate Challenge – Stage 1. (The U.S. Environmental Protection Agency et al, 2017)
[3] Including concentration polarization.

below the minimum gypsum induction time. In Sample B, silica's induction time[4] is shorter, so it is the scale that limits the additional recovery ratio to 74.5% of the RO concentrate flow rate. Calcite and other carbonates remain subsaturated throughout the entire concentration process, as the pH was reduced to 5 from the values in Table 5 values through acid addition (as seen in Figure 8). Therefore, $CaCO_3$ are not shown in Figure 9.

As each batch cycle progresses, the concentration of salts in contact with the membrane increases. The recovery ratios for Sample A and Sample B are chosen so that the batch process duration is shorter than the induction time of any common scalant.

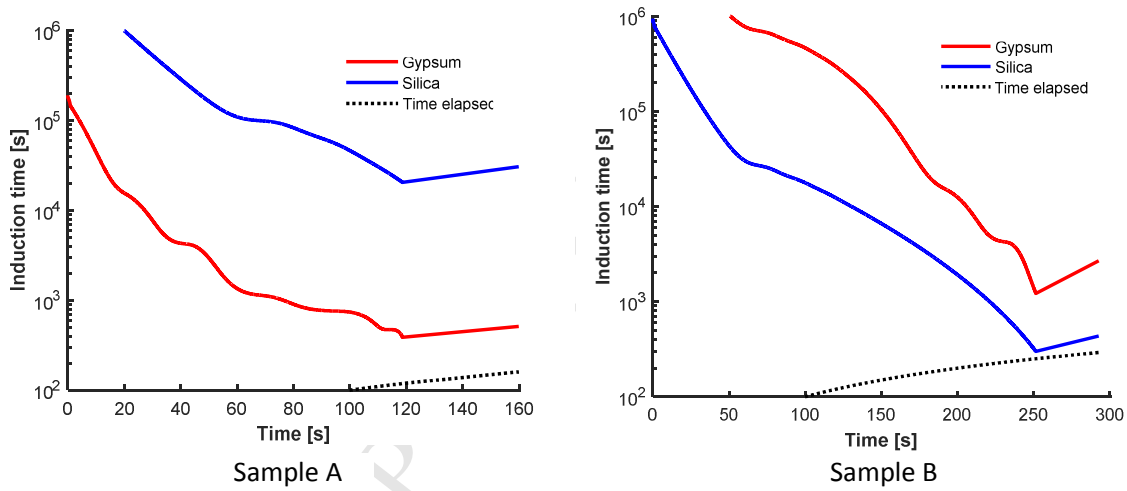

Figure 9. Induction time of Samples A and B over the course of a batch RO cycle. Induction time decreases as the salinity increases over the duration of a cycle.

Figure 10 shows the potential increase in total water recovery achievable by feeding the RO concentrate (sample A and B) to a batch RO system. The recoveries achieved are close to 90% for both samples.

[4] The jagged appearance of gypsum induction time curves results from the interpolation of induction time experimental data.

Additionally, as a result of increased water recovery, there is less concentrate to dispose of, which is especially beneficial when RO concentrate must be trucked away for disposal (Hutchings et al., 2010).

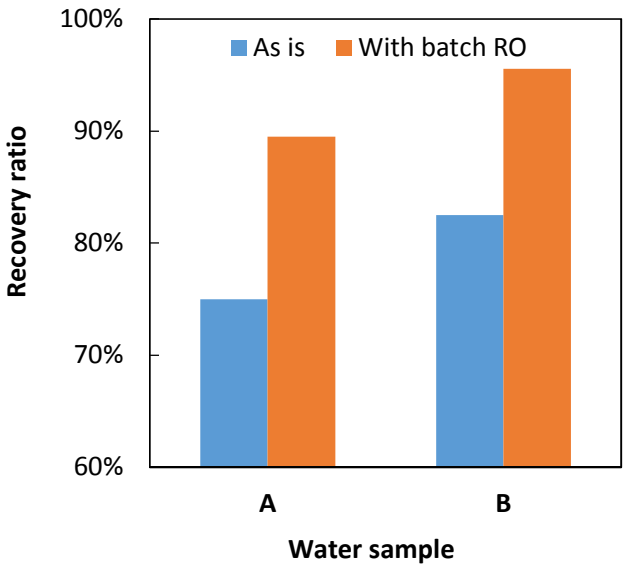

Figure 10. Potential for increased water recovery through acid addition and batch RO concentration.

4. Conclusions

This study developed and validated a simple method of predicting the occurrence of scaling in batch RO systems. The model equates the time delay of fouling to the nucleation induction time based on correlations from the literature. The model was validated against experimental data for fouling time delay in continuous RO and used to predict the increase in recovery ratio achievable through the use of batch RO with different water sources.

Through this study, the following conclusions were reached:

- The liquid residence times in batch (including semi-batch) RO are 3–4 orders of magnitude shorter than in continuous RO, which may explain batch systems' resistance to membrane fouling.
- Batch RO systems can treat water to higher recovery without scaling than continuous RO systems. For example, in systems limited by $CaSO_4$ scaling, batch operation can reach high recoveries (>90%) under conditions that limit continuous RO recovery to 60%.
- Batch operation has the potential to further concentrate brine from existing continuous RO plants and reduce the volume of concentrate disposal at inland water desalination plants.

5. Author contributions

David led the overall research effort, proposed the methodology, carried out modeling (Figs. 4-8), created most graphics (graphical abstract, Figs. 1, 2, 8), and wrote most manuscript sections. Emily provided modeling (Figs. 3, 9, and 10), experimental validation, and significant writing. Laith contributed to the modeling shown in Figs. 4 and 5. Grace assisted with modeling and writing the introduction. Jaichander contributed to the model evaluated in Figs. 3, 9, and 10 and performed PHREEQC modeling of saturation indexes. John guided the research effort.

6. Acknowledgements

EWT would like to thank The Martin Fellowship for Sustainability and acknowledge that this material is based upon work supported by the National Science Foundation Graduate Research Fellowship Program under Grant No. 1122374. The authors would like to thank Yvana Ahdab and Dr. Gregory P. Thiel for

their contributions related to the concentrations and saturation indexes of salts in standard bodies of water. LAM and GC thank the Undergraduate Research Opportunities Program at MIT for funding.

References

[Bartman et al., 2011] Bartman, A. R., Lyster, E., Rallo, R., Christofides, P. D., and Cohen, Y. (2011). Mineral scale monitoring for reverse osmosis desalination via real-time membrane surface image analysis. *Desalination*, 273(1):64–71.

[Bartman et al., 2009] Bartman, A. R., McFall, C. W., Christofides, P. D., and Cohen, Y. (2009). Model-predictive control of feed flow reversal in a reverse osmosis desalination process. *Journal of Process Control*, 19(3):433–442.

[Boo et al., 2012] Boo, C., Lee, S., Elimelech, M., Meng, Z., and Hong, S. (2012). Colloidal fouling in forward osmosis: role of reverse salt diffusion. *Journal of membrane science*, 390:277–284.

[Çelikbilek et al., 2012] Çelikbilek, M., Ersundu, A. E., and Aydn, S. (2012). *Crystallization Kinetics of Amorphous Materials*. INTECH Open Access Publisher.

[Chai et al., 2007] Chai, G.-Y., Greenberg, A., and Krantz, W. (2007). Ultrasound, gravimetric, and SEM studies of inorganic fouling in spiral-wound membrane modules. *Desalination*, 208(1-3):277–293.

[Chakraborty et al., 2015] Chakraborty, S., Gangasalam, A., Curcio, S., et al. (2015). Special issue: Green technologies for environmental pollution control and prevention. *Ecotoxicology and Environmental Safety*, 121:1–278.

[Chesters, 2009] Chesters, S. P. (2009). Innovations in the inhibition and cleaning of reverse osmosis membrane scaling and fouling. *Desalination*, 238(1):22–29.

[Cohen et al., 2017a] Cohen, B., Lazarovitch, N., and Gilron, J. (2017a). Upgrading groundwater for irrigation using monovalent selective electrodialysis. *Desalination*.

[Cohen et al., 2017b] Cohen, Y., Semiat, R., and Rahardianto, A. (2017b). A perspective on reverse osmosis water desalination: Quest for sustainability. *AIChE Journal*, 63(6):1771–1784.

[Cohen-Tanugi et al., 2014] Cohen-Tanugi, D., McGovern, R. K., Dave, S. H., Lienhard, J. H., and Grossman, J. C. (2014). Quantifying the potential of ultra-permeable membranes for water desalination. *Energy & Environmental Science*, 7(3):1134–1141.

[Comstock et al., 2011] Comstock, S. E. H., Boyer, T. H., and Graf, K. C. (2011). Treatment of nanofiltration and reverse osmosis concentrates: comparison of precipitative softening, coagulation, and anion exchange. *Water Research*, 45(16):4855–65.

[D. M. Warsinger, 2016] D. M. Warsinger, A. Servi, S.Van Belleghem, J. Gonzalez, J. Swaminathan, J. Kharraz, H. W. Chung, H. A. Arafat, K. K. Gleason, J. H. Lienhard V. (2016). Combining air recharging and membrane superhydrophobicity for fouling prevention in membrane distillation. *Journal of Membrane Science*, 505:241–252.

[Efraty, 2015] Efraty, A. (2015). CCD series no-16: opened vs. closed circuit SWRO batch desalination for volume reduction of silica containing effluents under super-saturation conditions. *Desalination and Water Treatment*, (ahead-of-print):1–16.

[Efraty et al., 2011] Efraty, A., Barak, R. N., and Gal, Z. (2011). Closed circuit desalination-a new low energy high recovery technology without energy recovery. *Desalination and Water Treatment*, 31(1-3):95–101.

[Efraty and Septon, 2012] Efraty, A. and Septon, J. (2012). Closed circuit desalination series no-5: high recovery, reduced fouling and low energy nitrate decontamination by a cost-effective BWRO-CCD method. *Desalination and Water Treatment*, 49(1-3):384–389.

[Elimelech et al., 1997] Elimelech, M., Zhu, X., Childress, A. E., and Hong, S. (1997). Role of membrane surface morphology in colloidal fouling of cellulose acetate and composite aromatic polyamide reverse osmosis membranes. *Journal of Membrane Science*, 127(1):101–109.

[Gal et al., 2016] Gal, Z., Septon, J., Efraty, A., and Lee, A.-M. (2016). CCD series no-20: high-flux low-energy upgrade of municipal water supplies with 96% recovery for boiler-feed and related applications. *Desalination and Water Treatment*, pages 1–9.

[Gomez-Morales et al., 1996] Gomez-Morales, J., Torrent-Burgues, J., and Rodriguez-Clemente, R. (1996). Nucleation of calcium carbonate at different initial ph conditions. *Journal of crystal growth*, 169(2):331–338.

[Greenlee et al., 2009] Greenlee, L. F., Lawler, D. F., Freeman, B. D., Marrot, B., and Moulin, P. (2009). Reverse osmosis desalination: water sources, technology, and today's challenges. *Water research*, 43(9):2317–2348.

[Gu et al., 2013] Gu, H., Bartman, A. R., Uchymiak, M., Christofides, P. D., and Cohen, Y. (2013). Self-adaptive feed flow reversal operation of reverse osmosis desalination. *Desalination*, 308:63–72.

[Gutentag et al., 1984] Gutentag, E. D., Heimes, F. J., Krothe, N. C., Luckey, R. R., and Weeks, J. B. (1984). *Geohydrology of the High Plains Aquifer in parts of Colorado, Kansas, Nebraska, New Mexico, Oklahoma, South Dakota, Texas and Wyoming*. US Government Printing Office Washington, DC.

[He et al., 1999] He, S., Kan, A. T., and Tomson, M. B. (1999). Inhibition of calcium carbonate precipitation in NaCl brines from 25 to 90°C. *Applied Geochemistry*, 14(1):17 – 25.

[He et al., 1994] He, S., Oddo, J. E., and Tomson, M. B. (1994). The nucleation kinetics of calcium sulfate dihydrate in NaCl solutions up to 6 M and 90 °C. *Journal of Colloid and Interface Science*, 162(2):297–303.

[Hoek et al., 2008] Hoek, E., Allred, J., Knoell, T., and Jeong, B.-H. (2008). Modeling the effects of fouling on full-scale reverse osmosis processes. *Journal of Membrane Science*, 314(1):33–49.

[Hutchings et al., 2010] Hutchings, N. R., Appleton, E. W., McGinnis, R. A., et al. (2010). Making high quality frac water out of oilfield waste. In *SPE Annual Technical Conference and Exhibition*. Society of Petroleum Engineers.

[Hydranautics, 2001] Hydranautics (2001). Theory & overview of reverse osmosis (RO).

[Jawor and Hoek, 2009] Jawor, A. and Hoek, E. M. (2009). Effects of feed water temperature on inorganic fouling of brackish water RO membranes. *Desalination*, 235(1-3):44–57.

[Kempter et al., 2013] Kempter, A., Gaedt, T., Boyko, V., Nied, S., Kley, M., and Huber, K. (2013). Controlling silica in water treatment applications. In *Proceedings of the International Desalination Association World Congress on Desalination and Water Reuse, Tianjin, China, Oct. 20-25*.

[Khan et al., 2014] Khan, M. T., Busch, M., Molina, V. G., Emwas, A.-H., Aubry, C., and Croue, J.-P. (2014). How different is the composition of the fouling layer of wastewater reuse and seawater desalination RO membranes? *Water Research*, 59(0):271 – 282.

[Kim et al., 2009] Kim, S., Lee, S., Lee, E., Sarper, S., Kim, C.-H., and Cho, J. (2009). Enhanced or reduced concentration polarization by membrane fouling in seawater reverse osmosis (SWRO) processes. *Desalination*, 247(1-3):162–168.

[Kumar et al., 2017] Kumar, R., Ahmed, M., Bhadrachari, G., and Thomas, J. P. (2017). Desalination for agriculture: water quality and plant chemistry, technologies and challenges. *Water Science and Technology: Water Supply*, page ws2017229.

[Malki, 2008] Malki, M. (2008). Optimizing scale inhibition costs in reverse osmosis desalination plant. *International Desalination And Water Reuse Quarterly*, 17(4):28.

[McGovern et al., 2016] McGovern, R. K. and Lienhard, J. H. (2016). On the asymptotic flux of ultrapermeable seawater reverse osmosis membranes due to concentration polarisation. *Journal of Membrane Science*, 520:560–565.

[McGovern and Lienhard, 2014] McGovern, R. K. and Lienhard, J. H. (2014). On the potential of forward osmosis to energetically outperform reverse osmosis desalination. *Journal of Membrane Science*, 469:245 – 250.

[Nagy and Braatz, 2012] Nagy, Z. K. and Braatz, R. D. (2012). Advances and new directions in crystallization control. *Annual review of chemical and biomolecular engineering*, 3:55–75.

[Parkhurst and Appelo, 2013] Parkhurst, D. L. and Appelo, C. (2013). Description of input and examples for PHREEQC version 3-a computer program for speciation, batch-reaction, one-dimensional transport, and inverse geochemical calculations. *US geological survey techniques and methods, book*, 6:497.

[Pomerantz et al., 2006] Pomerantz, N., Ladizhansky, Y., Korin, E., Waisman, M., Daltrophe, N., and Gilron, J. (2006). Prevention of scaling of reverse osmosis membranes by "zeroing" the elapsed nucleation time. part i. calcium sulfate. *Industrial & engineering chemistry research*, 45(6):2008–2016.

[Qi and Harris, 2017] Qi, S. and Harris, A. (2017). Geochemical database for the brackish groundwater assessment of the United States. *U.S. Geological Survey data release*.

[Qiu and Davies, 2012a] Qiu, T. and Davies, P. (2012a). Longitudinal dispersion in spiral wound RO modules and its effect on the performance of batch mode RO operations. *Desalination*, 288:1 – 7.

[Qiu and Davies, 2012b] Qiu, T. and Davies, P. A. (2012b). Comparison of configurations for high-recovery inland desalination systems. *Water*, 4(3):690–706.

[Ramon and Hoek, 2012] Ramon, G. Z. and Hoek, E. (2012). Osmotic backwashing of organic-fouled reverse osmosis membranes: Efficiency and implications for fouling control. In *ABSTRACTS OF PAPERS OF THE AMERICAN CHEMICAL SOCIETY*, volume 243. AMER CHEMICAL SOC 1155 16TH ST, NW, WASHINGTON, DC 20036 USA.

[Rezaei et al., 2017] Rezaei, M., Warsinger, D. M., Lienhard, J. H., and Samhaber, W. M. (2017). Wetting prevention in membrane distillation through superhydrophobicity and recharging an air layer on the membrane surface. *Journal of Membrane Science*, 530:42–52.

[Roy et al., 2017] Roy, Y., Warsinger, D. M., and Lienhard, J. H. (2017). Effect of temperature on ion transport in nanofiltration membranes: Diffusion, convection and electromigration. *Desalination*, 420:241 – 257.

[Sagiv et al., 2008] Sagiv, A., Avraham, N., Dosoretz, C. G., and Semiat, R. (2008). Osmotic backwash mechanism of reverse osmosis membranes. *Journal of Membrane Science*, 322(1):225–233.

[Salvador Cob et al., 2012] Salvador Cob, S., Beaupin, C., Hofs, B., Nederlof, M., Harmsen, D., Cornelissen, E., Zwijnenburg, A., Genceli Güner, F., and Witkamp, G. (2012). Silica and silicate precipitation as limiting factors in high-recovery reverse osmosis operations. *Journal of Membrane Science*, 423-424:1–10.

[Servi et al., 2017] Servi, A. T., Guillen-Burrieza, E., Warsinger, D. M., Livernois, W., Notarangelo, K., Kharraz, J., Lienhard, J. H., Arafat, H. A., and Gleason, K. K. (2017). The effects of iCVD film thickness and conformality on the permeability and wetting of MD membranes. *Journal of Membrane Science*, 523:470–479.

[Shirazi et al., 2010] Shirazi, S., Lin, C.-J., and Chen, D. (2010). Inorganic fouling of pressure-driven membrane processes – A critical review. *Desalination*, 250(1):236–248.

[Sonera et al., 2015] Sonera, V., Septon, J., and Efraty, A. (2015). CCD series no-21: illustration of high recovery (93.8%) of a silica containing (57 ppm) source by a powerful technology of volume reduction prospects. *Desalination and Water Treatment*, pages 1–9.

[Stover, 2012] Stover, R. (2012). Evaluation of closed circuit reverse osmosis for water reuse. In *Proc. 27th Annual Water Reuse Symp., Hollywood, FL, USA, September, Water Reuse Association, Paper B4–2*.

[Stover, 2013] Stover, R. L. (2013). Industrial and brackish water treatment with closed circuit reverse osmosis. *Desalination and Water Treatment*, 51(4-6):1124–1130.

[Swaminathan et al., 2017] Swaminathan, J., Tow, E. W., Warsinger, D. M., and Lienhard, J. H. (2017). Effect of practical losses on optimal design of batch RO systems. *IDA 2017 World Congress on Water Reuse and Desalination, São Paulo, Brazil, October 15-20, 2017. IDA Ref. no IDA17WC-58334-Swaminathan*.

[Tarquin and Delgado, 2012] Tarquin, A. and Delgado, G. (2012). Concentrate enhanced recovery reverse osmosis: a new process for RO concentrate and brackish water treatment. *Proc. American Institute of Chemical Engineers Meet., Pittsburg, PA, USA, October, American Institute of Chemical Engineers, Paper 272277*.

[The U.S. Environmental Protection Agency et al, 2017] The U.S. Environmental Protection Agency, the U.S. Army, U.S Army Corps of Engineers, and the Water Research Foundation (2017). More water less concentrate - stage 1. *BOR Innocentive Challenge, Challenge ID: 9933762*.

[Thiel and Lienhard, 2014] Thiel, G. P. and Lienhard, J. H. (2014). Treating produced water from hydraulic fracturing: Composition effects on scale formation and desalination system selection. *Desalination*, 346:54–69.

[Thiel et al., 2015] Thiel, G. P., Tow, E. W., Banchik, L. D., Chung, H. W., and Lienhard, J. H. (2015). Energy consumption in desalinating produced water from shale oil and gas extraction. *Desalination*, 366:94 – 112. Energy and Desalination.

[Tong et al., 2017] Tong, T., Zhao, S., Boo, C., Hashmi, S. M., and Elimelech, M. (2017). Relating silica scaling in reverse osmosis to membrane surface properties. *Environmental Science & Technology*, 51(8):4396–4406.

[Tow et al., 2015a] Tow, E. W., McGovern, R. K., and Lienhard, J. H. (2015a). Raising forward osmosis brine concentration efficiency through flow rate optimization. *Desalination*, 366:71 – 79.

[Tow et al., 2015b] Tow, E. W., McGovern, R. K., and Lienhard, J. H. (2015b). Raising forward osmosis brine concentration efficiency through flow rate optimization. *Desalination*, 366:71 – 79. Energy and Desalination.

[Tow et al., 2016] Tow, E. W., Rencken, M. M., and Lienhard, J. H. (2016) In situ visualization of organic fouling and cleaning mechanisms in reverse osmosis and forward osmosis. *Desalination,* 399:138–147.

[Tow et al., 2017] Tow, E. W., Warsinger, D. M., Swaminathan, J., Trueworthy, A. M., Thiel, G. P., Zubair, S. M., Myerson, A. S., and Lienhard, J. H. (2018). Comparison of fouling propensity between reverse osmosis, forward osmosis, and membrane distillation. *In preparation*.

[Waly et al., 2009] Waly, T., Kennedy, M. D., Witkamp, G. J., Amy, G., and Schippers, J. C. (2009). Will calcium carbonate really scale in seawater reverse osmosis? *Desalination and Water Treatment*, 5(1-3):146–152.

[Warsinger et al., 2015a] Warsinger, D. M., Gonzalez, J. V., Van Belleghem, S. M., Servi, A., Swaminathan, J., and Lienhard, J. H. (2015a). The combined effect of air layers and membrane superhydrophobicity on biofouling in membrane distillation. *Proceedings of The American Water Works Association Annual Conference and Exposition, Anaheim, CA, USA*.

[Warsinger et al., 2015b] Warsinger, D. M., Mistry, K. H., Nayar, K. G., Chung, H. W., and Lienhard, J. H. (2015b). Entropy generation of desalination powered by variable temperature waste heat. *Entropy*, 17:7530–7566.

[Warsinger et al., 2015c] Warsinger, D. M., Nayar, K. G., Tow, E. W., and Lienhard, J. H. (2015c). Efficiency and fouling of closed circuit reverse osmosis and a novel variant: Pushing the limits on desalination efficiency. In *Oral Presentation, New England Graduate Student Water Symposium (NEGSWS), Amherst, MA, USA*.

[Warsinger et al., 2017a] Warsinger, D. M., Servi, A., Connors, G. B., Mavukkandy, M. O., Arafat, H. A., Gleason, K., and Lienhard, J. H. (2017a). Reversing membrane wetting in membrane distillation: comparing dryout to backwashing with pressurized air. *Environmental Science: Water Research & Technology*, 3:930–939.

[Warsinger et al., 2015d] Warsinger, D. M., Swaminathan, J., Chung, H. W., Jeong, S., and Lienhard, J. H. (2015d). The effect of filtration and particulate fouling in membrane distillation. In *Proceedings of The International Desalination Association World Congress on Desalination and Water Reuse, San Diego, CA, USA, IDAWC15- Warsinger-51667*.

[Warsinger et al., 2015e] Warsinger, D. M., Swaminathan, J., Guillen-Burrieza, E., Arafat, H. A., and Lienhard, J. H. (2015e). Scaling and fouling in membrane distillation for desalination applications: A review. *Desalination*, 356:294–313.

[Warsinger et al., 2017b] Warsinger, D. M., Swaminathan, J., and Lienhard, J. H. (2017b). Ultrapermeable membranes for batch desalination: maximum desalination energy efficiency, and system cost. *IDA 2017 World Congress on Water Reuse and Desalination, São Paulo, Brazil, October 15-20, 2017*.

[Warsinger et al., 2014] Warsinger, D. M., Swaminathan, J., and Lienhard, J. H. (Kyoto, Japan August 2014). Effect of module inclination angle on air gap membrane distillation. In *Proceedings of the 15th International Heat Transfer Conference, IHTC-15, Paper No. IHTC15-9351*.

[Warsinger et al., 2016a] Warsinger, D. M., Tow, E. W., and Lienhard, J. H. (2016a). Inorganic fouling resistance of membrane distillation vs. reverse osmosis. In *Proceedings of Singapore Water Week 2016 (SIWW), Singapore*.

[Warsinger et al., 2016b] Warsinger, D. M., Tow, E. W., Nayar, K., Masawadeh, L. A., and Lienhard, J. H. (2016b). Energy efficiency of batch and semi-batch (CCRO) reverse osmosis desalination. *Water Research*, 106:272–282.

[Warsinger et al., 2017c] Warsinger, D. M., Tow, E. W., Swaminathan, J., and Lienhard, J. H. (2017c). Theoretical framework for predicting inorganic fouling in membrane distillation and experimental validation with calcium sulfate. *Journal of Membrane Science*, 528:381 – 390.

[Warsinger and Tow, 2016] Warsinger, D. M. and Tow, Emily W. Lienhard, J. H. (2016). Enhancing energy efficiency of reverse osmosis with batch and semi-batch processes. In *Oral Presentation, 9th International Conference on Desalination, November 13-15, Yas Island, Abu Dhabi, UAE*.

[Xie et al., 2015] Xie, M., Lee, J., Nghiem, L. D., and Elimelech, M. (2015). Role of pressure in organic fouling in forward osmosis and reverse osmosis. *Journal of Membrane Science*, 493:748 – 754.

[Xyla et al., 1992] Xyla, A. G., Mikroyannidis, J., and Koutsoukos, P. G. (1992). The inhibition of calcium carbonate precipitation in aqueous media by organophosphorus compounds. *Journal of Colloid and Interface Science*, 153(2):537–551.

[Yang, 2005] Yang, N. (2005). Physical Conditioning for Scale Prevention during Desalination by Reverse Osmosis. *Master's Thesis: Chalmers Institute of Technology, Goteborg, Sweden*.